Tribological, Thermal and Corrosive behaviour of aluminium alloy 2219 reinforced by Si3N4 nanosized powder

Manjunatha C J (manjunathacj79@gmail.com)
Sha-Shib College of Engineering
B. Venkata Narayana
SEA College of Engineering and Technology
D Bino Prince Raja
SJCIT: SJC Institute of Technology
Rimal Isaac R S
Noorul Islam College of Engineering: Noorul Islam Centre For Higher Education

Research Article

Keywords: Si3N4, Thermal Analysis, Wear, Corrosion Analysis, SEM

Posted Date: April 6th, 2021

DOI: https://doi.org/10.21203/rs.3.rs-346775/v1

Abstract

The MMC technique is the most effective contrast method when compared with other techniques. By using the method of high energy stir casting, Aluminium alloy Al2219 is reinforced with various percentages of Si3N4 (0, 3, 6, and 9%) particles. X-ray diffraction along with Scanning electron microscope was performed to characterize the composite. The mechanical and thermal behaviours such as differential thermal analysis thermo gravimetric analysis/, tensile , wear and hardness behaviours were investigated. By using electro chemical potentiodynamic polarization test, the consequence of heat treatment on the corrosion behaviour of the composites when compared to its matrix in 3.5 % NaCl when at 600 rpm was also investigated. In this experimental study, the wear of the aluminium composites was significantly decreased on addition of Si3N4 particles. The study also revealed that, since the inclusion of Si3N4 in the samples and compared to the base aluminium alloy, the mechanical properties of the composites, such as wear resistance , hardness and tensile strength increased by percentage. The surface morphology and Scanning electron microscope analysis of worn surfaces in the test pieces unfold that with the increase in reinforcement content, wear rate decreases.

Introduction

In the recent times, the technology space in aircraft, aerospace, and automotive industries is rapidly advancing which in turn increases the demand for composite materials which is widely being used in the above-mentioned areas. The special properties of Composites materials such as low specific gravity makes the material highly superior in modulus and strength when compared with most traditional engineering metallic materials [1].

Metal matrix composites are explicitly utilized composite materials which is made with generally wo constituents, one of the constituents is a metal matrix and the other material is a reinforcement. In all the cases, the matrix is outlines with a metal and the use of pure metal as a matrix is mostly avoided. In general, the matrix is constituted by the use of an alloy. The general synthesis of the composite involves the mixing of the matrix and the reinforcement together.

Aluminium is extensively used in matrix material composites (MMCs). This is main reason for this is the unique features of aluminium such as good mechanical properties, low density, good machinability properties, low electrical resistance, high strength and good corrosion resistance. Although comparatively substandard wear resistance of these alloy has restrained its use in specific tribological applications. In the recent studies, both particulate and fibre reinforced aluminium alloy composites fabricated have shown appreciable improvement in their tribological properties, including but not limiting to sliding wear, seizure resistance, friction, and abrasive wear [3]. The production and utilization of Si_3N_4 was stimulated by increasing demand for low-cost reinforcement [9].

Wear based damages to the material is an important aspect in tribology buy even though it is highly important, it is one of the least understood field. It is also a youngest topic, lubrication, friction and wear

which needs more scientific attention. The practical significance of the same is being identified through the years [15].

Wear is responsible for a huge annual outlay by the consumers as well as the industries. Most of this goes in replacing or repairing equipment's that is worn out and does no longer perform its function. [7]. In many parts of the machine the damage is seen only after a percentage of the entire volume of the part has worn out. [14].

Number of studies have been conducted to characterize tribological behavior of Aluminium-based MMC. Suresh and Sridhara [16] reported on the impact of Gr and SiC (up to 10% wt%) on the wear properties of LM25-based aluminium composites. It was discovered that increasing the weight fraction of reinforcement particle in MMC reduced wear until it reached 7%, after which it increased. Wear of matrix material composites increased with increasing load due to an unstable tribo-layer, but decreased with increasing speed due to the presence of MML [17]. The effect of SiC and B_4C on the wear efficiency of the Al7075-based MMC was studied by Uvaraja and Natarajan [29]. Wear rate was found to decrease as the volume fraction of reinforcement, speed, and time increased, whereas it increased as the applied load increased. The reinforcement content was found to be the most important factor, followed by the applied load and sliding speed. Surface morphology and SEM analysis of the test pieces' worn surfaces showed that the wear rate decreased as the reinforcement material increased. The EDS findings were used to classify the MML that forms on the test specimen's worn surfaces. [17] [22]

The effects of reinforcement on composite corrosion activity are still unknown. It has been found that in the presence of reinforcement, the corrosion current density rises, decreases, or remains unchanged. Furthermore, reinforcement has been shown to influence the open circuit potential (OCP) by increasing, decreasing, or having no effect [24]. Heat treatment results are discovered to be a crucial factor in evaluating the corrosion behaviour of aluminium alloy composites. Kolman and Butt [25] examined the corrosion properties of an aluminum–silicon alloy composite reinforced with in-situ TiB_2 particulate after heat treatment. It was discovered that as the amount of TiB_2 in these composites increased, their corrosion resistance decreased. The effect of heat treatment of the reinforcing BN, Al_2O_3, and Ti (C, N) particles in the EN AW–AlCu4Mg1(A) aluminium alloy on its corrosion resistance in the presence of NaCl water solution was investigated by Wodarczyk-Fligier et al. [27]. The corrosion resistance of composite material heat treated in a 3 percent NaCl solution was found to be noticeably improved.

In the frame of reference of the discussion above, the aim of the current investigation is to study the morphological, mechanical and metallurgical properties of Si_3N_4 reinforced Aluminium Alloy AA2219. The reinforcement is embeded by high energy stir casting method with various percentage of Si_3N_4 (0,3,6 and 9) particles. The structural characterization was carried out by SEM, XRD and tests. Tensile, hardness and corrosion test are carried out for determining the mechanical behaviour of this material. TGA analysis has been carried out as thermal analysis**.** The wear behaviour of AA2219/ $\boldsymbol{Si_3N_4}$ MMC has not been explored so far and they are fabricated by two-step stir casting method. Characterization of microstructure and worn surface morphology of the composites was done by Scanning electron

microscope (SEM). Tensile fractured samples were made to undergo fractography study. Mechanically mixed layer (MML) of the test specimens were evaluated by EDS.

Experimental Aspects

Casting process

In this study the electrical furnace setup was replaced with a stir set up by using a simple blower furnace and the vertical drilling machine assembly as shown in the Fig. 1. As the high operating cost of electrical furnace is annihilated, the variable speed of drilling machine is obtained using the stirrer. The addition of Si_3N_4 particles in terms of ratio was done at 0, 3, 6, and 9% by the overall weight. Formulation process begins with the stirring out in a graphite crucible in a coal-fired furnace. Ceaseless stirring of the molten metal-matrix gives homogeneous mixture of the composite. This is instantly poured into the mould to get solidified. For melting the alloy Coal was used as a fuel. Al2219 was kept in a crucible and liquefied by melting it in a blower furnace at a temperature of 670 ℃ for 15 min. The Si_3N_4 powder was preheated to a temperature of 670°C using a separate muffle furnace. The temperature of the furnace was first increased above the temperature of the liquid.

Tensile test.

Ductile test examples were made according to the ASTM standard and tried in a Universal Testing Machine. In request to gauge the rigidity of the examples, they were made in a round and hollow shape as per ASTM E8. The information estimations of the four examples acquired from the ductile test were utilized. The fortifying stage in the metal network composites bears a huge division of the worry as it is commonly a lot stiffer than the grid. The molecule joining brings about an expansion in the work solidifying of the material. The higher work solidifying rate saw in the composites is because of the mathematical imperatives forced by the presence of the support. The expanding weight % of Si_3N_4 builds the work solidifying rate. The tensile samples before and after test is shown in figure 2 (a) and (b).

Hardness test.

The composites materials hardness was estimated by utilizing a Brinell hardness machine following the ASTM E10 standard. All the examples were applying a heap of 500 to 3000kgf for a time of Ten seconds. The test was done at room temperature and the estimation of hardness was taken at 3 distinct areas to keep away from the conceivable impact of indenter laying on the hard support particles. The midpoints of the apparent multitude of four readings were accounted for.

Pin-on-disc experimental set up

A pin-on-disc equipment is used to carry out the experiment which is coupled with a wear monitor and type friction with a data acquisition system. The above setup is used in measuring the wear behavior of composite by testing it against the hardened ground steel disc (EN-24) which is has a hardness value of

65HRC and surface roughness (Ra) of 0.5µm. the equipment is highly versatile which is designed in such a way to study the wear characteristics only under sliding conditions. In the equipment, sliding usually occurs between the rotating disc and the stationary pin. A D.C motor was used to rotate the disc; the motor is having a speed range of 100-1500 rpm with wear track diameter (50mm*160mm), which would yield sliding speed 0 to 10m/sec. The load has to be applied on pin sample (specimen) by deadweight through a pulley string arrangement. The system's maximum loading capacity is 100N. Fig 3 (a) & (b) shows Wear specimens before and after test.

TGA

Differential thermal analysis (DTA) and thermogravimetric analysis (TG) were carried out simultaneously using a TG/DTA EXSTAR 6300 instrument (SII Nanotechnology Inc.). Approximately 10 mg of the specimen is weighed on the alumina crucible and heated from 30 to 800 ℃ in a flow of air atmosphere (100 ml/min). The heating rate was 10 ℃/min. α-Alumina was used as reference standard.

XRD

XRD is commonly utilized to assess the samples' purity, phase and crystal structure [24]. Phase analysis of prepared specimens was done by XRD model D2 PHASER (Bruker AXS) using Cu/Kα radiation (λ = 1.54060 Å). Over the 2θ range of 20º-80º with a step size of 0.02º, peak values were obtained. All four samples have significant diffraction peaks that could be attributed to the Cu and W structures.

Characteristics peaks has been observed in the XRD pattern, and the relative intensity rate corresponding to the samples.

Corrosive test

Corrosion measurement were carried out using CHI 604D Electrochemical Workstation (CH Instruments, Inc) in 3.5% NaCl Solution using an Ag/AgCl reference electrode and platinum wire as a counter electrode. The Inhibitive efficiency is calculated using the below equation.

$$Inhibition\ Efficiency\ = \frac{C_{ra} - C_{rs}}{C_{ra}} \times 100$$

In the above equation for Inhibition Efficiency, C_{ra} denotes the corrosion rate of the unreinforced Al2219 alloy and C_{rs} is used to denote the corrosion rate of Al2219 alloy reinforced with Si_3N_4. Each run's output consists of a polarisation curve from which the corrosion parameters can be calculated using a manufactured software package using the Tafel extrapolation technique. The samples are shown in figure 4.

Result And Discussion

4.1 Effect of Tensile Analysis

Mechanical conduct of the composites was explored by pliable tests which are done utilizing a mechanized widespread malleable testing machine. The examples when the ductile test has appeared in Fig. 5. Four test examples were utilized for each run. The malleable properties, for example, rigidity, extreme elasticity, and modulus were deciphered from the pressure strain bends spoke. It is additionally obvious from the malleable test that expansion in the measure of support builds the elasticity, whereas there exists a lessening in pliability huge enhancement in the mechanical properties of the composite as contrasted and the Al2219 can be ascribed to the Si_3N_4.

The tensile tested specimen of AA2219 alloy with 0%, 3%, 6% and 9% of Si_3N_4 reinforced composite is subjected to fracture morphology and the result is as shown in Fig. 6 (i-iv). It has been noted that sample with 3% wt demonstrated a high breakage point. Scanning electron microscope image of AA2219 alloy in the Fig. 6 (i-iv) unravels that the AA2219 alloy has equally distributed, large voids, with a good number of comparatively equalled fibrous ligaments and dimples present on its surface. This discloses the ductile mode of the fracture. The composites 0%, 3%,6% and 9% of Si_3N_4 as shown in figure are small and minimal. Within the dimples the Si_3N_4 particles are excellently harboured. This confirms a good bonding between the matrix and the Si_3N_4 [30]. Because of the existence of Si3N4 particles, the dimples were found to be much shallower, and their size was decreased by growing a fraction of Si_3N_4 particles. This shows that the particles are uniformly distributed and strongly bound to the matrix. Despite the fact that fracture morphology shows signs of ductile fracture, ductile fracture is heavy in the AA2219 alloy and low in the composite. These fractography clearly demonstrate that the matrix and reinforcement have a strong bond, resulting in improved composite hardness and ultimate tensile strength [13, 30]. It confirms that as the percentage of Si_3N_4 increases, the percent of elongation decreases. This is mostly due to the Si_3N_4 particle's hardness. Many other researchers have found similar patterns [1, 13, 20, 30].

4.2 Brinell Hardness Analysis

The after-effects of Brinell hardness tests directed on AA2219 and the composite containing diverse wt. % of Si_3N_4 particles have appeared in Fig.7. They uncover critical improvement in the hardness with the expansion of Si_3N_4 fortification in the AA2219. The AA2219 composite with hardness esteem 63.71 HV and the aluminium-based composite containing 2 wt. % Si_3N_4 demonstrates 65.39 HV and this goes with expanding Si_3N_4 content. It is seen that the hardness of 10% Si_3N_4 is expanded by 73.93 HV more than AA2219. A striking accent in the hardness of the composite network can be seen with the expansion of Si_3N_4 particles. Hardness esteem uncovers that the higher estimation of hardness demonstrates the presence of Si_3N_4 particulates in the lattice composites. A hard fortification is consolidated into a delicate material; the hardness of the grid material is enhanced. Consequently, expanding the wt. % of Si_3N_4 builds the hardness of the composites.

4.3 Effect of Wear Analysis

Load (N)	Sliding Speed (Rpm)	Wear Rate in 10^{-7} mm^3/Nm			
		Wt.% of Si_3N_4			
		0	3	6	9
20	300	1.527	1.319	1.041	1.180
	600	1.562	1.388	1.145	1.249
	900	1.666	1.458	1.272	1.342
40	300	2.013	1.527	1.458	1.527
	600	2.326	2.152	1.701	1.874
	900	2.430	2.360	1.944	2.129

Table 1 Wear rate of all the samples with 20KN and 40KN Load

The above fig 8 shows Effect of wt. % of Si_3N_4 and sliding speed on wear behaviour of the AA2219/Si_3N_4 composites at 20N. Table 1 shows the Wear rate of all the samples with 20KN and 40KN Load

The above Fig 9 shows the Effect of wt. % of Si_3N_4 and with sliding speed of disk on wear behaviour of the Al2219/Si_3N_4 composites at 40N.The effect of Silicon Nitride (Si_3N_4) content on the wear characteristics of AA 2219/Si_3N_4 particulate for a wear test the loads of 20, and 40N and rotational speed of 300, 600, and 900 rpm as shown in Fig 7 and 8 which is the representative graphs plotted based on wear rate results. The following is revealed by the study of these Figures. The wear rate of the AA 2219/Si_3N_4 composites depends on the % of Silicon Nitride (Si_3N_4) dispersion. With the increase in Silicon Nitride (Si_3N_4) content from 3 to 6 wt. % wear rate was found to be decreased. But there is a result of an increase in wear rate for the 9 wt. % of Silicon Nitride (Si3N4) when compared with the 6 wt. % reinforcement. The weighted rate by wear is minimum for the composite containing 6 wt. % Silicon Nitride (Si_3N_4) dispersed in the as-cast as observed. At lower loads, the wear rate of the material remained almost constant with an increase in rpm. When comparing the results, the light wear rate was shown by AA2219 without dispersoid loss decreased in a steady manner. Perhaps, due to hard particles of Silicon Nitride (Si_3N_4) dispersed in the base matrix there is relatively rapid attainment of stability in the wear resistance, as seen in the above figures.

4.4 *Worn out surface analysis of Wear specimens*

Figure 10 (a) – (d) shows the surfaces of samples as viewed using a SEM which is cast Al2219 alloy and Al2219-3,6,9 wt. % Si_3N_4 composites after applying a load of 20N, 40N and 300, 600, 900rpm sliding speed test. Figure 10 (a) shows that some of the regions are damaged as seen in as cast Al2219 alloy. When higher load was applied, the degree of grooves formed at the worn surface of the matrix alloy is quite larger which causes a severe plastic deformation which causes severe wear in the specimens.

Figure 5.2, 5.3, 5.4 shows the amount of grooving in the surfaces of the Al2219 alloy composite. The grooves reduce as a result in the increase content of Si_3N_4 showing the lower material removal in comparison with Al2219 base matrix material.

4.5 XRD Investigations:

Fig- 11(a) shows the X-ray patterns of extracted AA2219 as cast composites. The fabricated AA 2219's X-ray diffraction pattern. The presence of aluminium (Al) and copper (Cu) of metallic compounds was discovered through the study of XRD peaks. The diffraction pattern clearly indicates Si_3N_4 particles, as shown in Fig. 11(b, c, and d). The relative fractions of the strength of the Si_3N_4 particles were measured. The relative fractions of Si_3N_4 particles found strength in the XRD pattern, with the highest peak occurring at the reinforcement particles. The particle peaks within the composite are visible using XRD. As the number of Si_3N_4 particles increases, the probability of reinforcement agglomeration in the AA 2219 matrix increases. The results show that metallic elements are present in the highest peaks and reinforcement is present in the lowest peaks. The relative strength occurs at a 38-degree angle, with strong peaks for wt% of composites. The percentage of Si_3N_4 in composites has been found to increase, resulting in a higher peak intensity level in the study.

4.6 TGA Analysis

Analyzing the thermal response of unreinforced Al2219 and developed Al2219- Si_3N_4 composites as shown in Figure 12 (a-d), has been established using a differential thermal analyzer (DTA) and thermogravimetric analyzer (TGA). The results from the thermograms shows that as the composite with incorporated Si_3N_4 has enhances the thermal stability of the aluminium alloy matrix. Apart from increase in inhibition efficiency, the addition of the nanoceramic Si_3N_4 also causes a decrease in the mass loss as the composite is heated from 30 ℃ to 800 ℃, which is clearly evident from the TG/DTA result. From the graph, there was a 7.3 % loss of mass for the unreinforced Al2219, whereas the addition of the incorporation of Si_3N_4 decreased the mass loss to 2.5% in 3 wt% Si_3N_4 reinforced alloy. At 6 wt %-Si_3N_4, the material was about 4.4% and mass loss was observed in 9 wt% particulates with an 7.6% loss. This shows the positive effect of the inclusion of the Si_3N4 helped in material saving for high temperature application by enhancing the reduction of mass loss with an optimal Si_3N_4 amount of 3%.

4.7. Corrosion

Sample	Corrosion Rate (mil/year)	Inhibition Efficiency (%)
0%	455.70	12.2
3%	346.20	24.03
6%	367.00	19.46
9%	170.60	62.56

Table 2: The corrosion behaviour of materials has been studied using Electrochemical workstation.

Figure 13 shows the potentiodynamic polarization graph for the Al 2219 allow with and without Si_3N_4 reinforcement. From the results, the corrosion rate and the inhibition efficiency were calculated and is shown in Table 2. the results clearly shows that the corrosion rate decreases as with the addition of Si_3N_4 which shows its positive effect on the material in preventing it from getting corroded. The inert properties of the nano ceramic Si_3N_4 that makes it resistant to corrosion was seen to influence the composite to have a low corrosion rate, its positive effect on the corrosion inhibition efficiency increases as the Si_3N_4 percentage increases from 3% to 9%.

Conclusion

The Tribological, thermal, morphological and mechanical characteristics of AA2219 with four wt% of Si_3N_4 composite was made by stir casting method. The study revealed the following results:

- Due to the dispersion of Si_3N_4 particles over the Aluminium alloy 2219 matrix increases the hardness value of the composites. Tensile strength reveals that increase firstly from 0-6% $Si_3N_4$and decreases suddenly at 9% Si_3N_4. HBW of the material gradually increases as percentage composition of aluminium varies from 0% to 6% Si_3N_4 and decreases in 9% of Si_3N_4. Tensile strength of AA2219-Si_3N4 composite revealed that high strength is obtained at 6%wt addition of Si_3N4 when compared to other the weight percentage. The intensity of facts initial will increase from 0% to 6% and then suddenly to 9%. The results of the tests like hardness and tensile increased with increasing the wt% of Si_3N_4 in AA2219 composites [10]
- The XRD analysis of Al 2219 alloy / Si_3N_4 composites reexhibits the aluminium, Silicon Nitride (Si_3N_4) and intermetallic (Al-Cu)
- The tribological characteristics – mass wear, friction force and coefficient of friction, of the AA2219-Si_3N_4 composites increases with the 9% of Si_3N_4 The load factor and sliding speed is the controlling or dominated factor for wear tests, with increase in loads and speeds of sliding over the sample leads to significant increase in overall wear rate of the material. The AA2219-with-3, 6, and 9 wt. % of Si_3N_4 composites has shown the lower rate wear compared to the original AA2219 alloy matrix. Work concluded that the 9% of Si_3N_4 reinforcement is better for the wear resistances at minimum load applications of Aluminium alloy 2219 matrix materials. Work concluded that the minimum 6% of Si_3N_4 reinforcement is better for the wear resistances at maximum load applications of Aluminium alloy 2219 matrix materials.
- The wear rate is dominated by load factor and sliding speed. The increase in loads and sliding speeds leads to a significant increase in the wear rate. The AA2219-3, 6, and 9 wt. % of $\boldsymbol{Si_3N_4}$ composites have shown a lower rate of wear as compared to that observed in the as-cast AA2219 alloy matrix. For better wear resistance at the minimum load of application in Aluminium alloy 2219 matrix materials, the maximum amount of 9% of $\boldsymbol{Si_3N_4}$ reinforcement is to be suggested. For better

wear resistance at the Maximum load of application in Aluminium alloy 2219 matrix materials, the minimum amount of 6% of Si_3N_4 reinforcement is to be suggested.

- The coefficient of friction and wear rate the of Al/ Si_3N_4 MMC was found to be lower than that of AA2219. The smaller and finer grain size, improved hardness, reduction in the porosity level and uniform distribution of Si_3N_4 particles are the various reasons for this. When the wt.% of Si_3N_4 content increase the wear rate is found to be decreased with an increase in sliding velocity [23]
- The worn area shows a rough wear process, which is mainly the product of hard particulate exposure. In the case of AA2219/ Si_3N_4 Composites, the particulate inhibits delamination progression, while the wear resistance is supplemental.
- The corrosion resistance of the matrix alloy was improved when Si_3N_4 particles were added in a quantity of up to 9% by weight. The AA2219- Si_3N_4 alloy matrix composite showed high corrosion resistance with corrosion rates of 367.00 mil/year for 6 wt% Si_3N_4 and 60 mil/year 9 wt% Si_3N_4. Heat treatment of the composites and matrix alloy improved corrosion and wear resistance.

Declarations

Funding statement: NIL

Conflict of Interest: No Conflict of interest

Author contributions: Equal Contribution

Availability of data and material: I Can provide as per the request

Compliance with ethical standards: yes

Consent to participate: Yes

Consent for Publication: Yes

Acknowledgments: Yes

References

[1] Siddeshkumar N G, G S Shiva Shankar &S.Basavarajappa,“Comparative Study on Dry Sliding Wear Behaviour of Metal Matrix Hybrid Composites at Room and High Temperature Conditions”, International Journal of Engineering Research & Advanced Technology,**1** (2015)16-24.

[2] T. Dileep and P. N. S. Srinivas,Enhancement Of Mechanical, Microscopic And Tribological Properties Of Hybrid Metal Matrix Composite Reinforced With Alumina, Graphite And Silicon Carbide, International Journal of Latest Engineering Research and Applications,**1**, (2016) 41-49.

[3] Jayasheel I. Harti1, B. R. Sridhar , H. R. Vitala, and Pankaj R. Jadhav, “Wear Behavior of Al2219-TiC Particulate Metal Matrix Composites” American Journal of Materials Science, **5** (2015), 34-37.

[4] Siddesh kumar N G**,** V M Ravindranath,G S Shiva Shankar “ Mechanical and wear behavior of aluminium metal matrix hybrid composites” procedia material science,**5** (2014) 908-917.

[5] Veeravalli Ramakoteswara Rao, Nallu Ramanaiah, Mohammed Moulana Mohiuddin Sarcar, “Mechanical and tribological properties ofAA7075–TiC metal matrix composites under heat treated (T6) and cast conditions” JMRTEC, (2016)1-7.

[6] Rajesh Agnihotri and Santosh Dagar, Mechanical Properties of Al-SiC Metal Matrix Composites Fabricated by Stir Casting Route, Res Med Eng Sci, (2017)1-6.

[7] L. Prince Jeya Lal, R. Manigantan, Suryanarayan. C.P, Experimental Study of Wear Rate Coefficient of Aluminium Hybrid Composites Manufactured By Stir Casting Technique, **3**, (2016)17-20.

[8] S. Suresh, N. Shenbaga Vinayaga Moorthi, N. Selvakumar, S. C. Vettivel, Tribological Tensile and Hardness Behavior Of TiB_2 Reinforced Aluminium Metal Matrix Composite, Journal of the Balkan Tribological Association **20**, (2014),380–394.

[9] Manjunatha C J, and B.Venkata Narayana, Experimental Analysis of mechanical properties of Aluminium Alloy 2219 reinforced with Si_3N_4, International Journal of Innovative Technology and Exploring Engineering, 9, (2019) 504-508.

[10] A. Baradeswaran, A. Elayaperumal, J. Paulo Davim: Effect of B4c On Mechanical Properties And Tribological Behaviour Of Al6061–B4c Composites, J Balk Tribol Assoc, **19**, (2013).

[11] Y. Kayali: Wear And Corrosion Behaviour Of Borided And Nitrided M2 High Speed Steel, J Balk Tribol Assoc, **19**, (2013).

[12] I. Sulima, L. Jaworska, P. Wyzga, M. Perek-Nowak: The Influence Of Reinforcing Particles On Mechanical And Tribological Properties And Microstructure Of The Steel–Tib2 Composites, J Achiev Mater Manuf Eng, **48**, (2010).

[13] Pengting Li, Yunguo Li, Yuying Wu, Guolong Ma, Xiangfa Liu: Distribution Of Tib2 Particles And Its Effect On The Mechanical Properties Of A390 Alloy. Mater Sci Eng A, **546**, (2012).

[14] A. Sreenivasan, S. Paul Vizhian, N. D. Shivakumar, M. Muniraju, M. Raguraman: A Study Of Micro Structure And Wear Behavior Of Tib2/Al Metal Matrix Composites, Solids Struct, **8**, (2011).

[15] I. Gunes, A. Dalar: Effect Of Sliding Speed On Friction And Wear Behaviour Of Borided Gear Steels. J Balk Tribol Assoc, **19,** (2013).

[16] Amit Sharma, R. M. Belokar, Sanjeev Kumar, 2018, *Journal of the Brazilian Society of Mechanical Sciences and Engineering* ***40*** *294*

[17*]* Suresha S, Sridhara BK 2010, *Compos Sci Technol* **70** 1652

[18] Uvaraja VC, Natarajan N 2012. *J Miner Mater Charact Eng* **11** 757

[19] S. Suresh a,n , N. Shenbaga Vinayaga Moorthi b , S.C. Vettivel c , N. Selvakumar d,3 , G.R. Jinu 2014, *Material Science & Engineering* A **612** 15

[20] E.P. Sreedev, H.K. Govind, A. Raj P, S. Adithyan, H.A. Narayan, K.V. Shankar, M. Balachandran, 2020, *Tribology in Industry* **42** 299

[21] L.V. Priyanka Muddamsetty, N. Radhika, 2016, *Tribology in Industry* **38** 108

[22] P.V. Reddy, Kumar, G. S., D.M. Krishnudu, H.R. Rao, 2020, *Journal of Bio- and Tribo-Corrosion* **6**

[23**]** Nunes PCR, Ramanathan LV (1995) Corrosion behavior of alumina-aluminum and silicon carbide-aluminum metal matrix composites. Corrosion 51:610

[24] Toptan F, Alves AC, Kerti I, Ariza E, Rocha LA (2013) Corrosion and tribocorrosion behavior of Al–Si–Cu–Mg alloy and its composites reinforced with B4C particles in 0.05 M NaCl solution. Wear 306:27

[25] Kolman DG, Butt DP (1997) Corrosion behavior of a novel SiC/ Al2O3/Al composite exposed to chloride environments. J Electrochem Soc 144:3785

[26] Sun HH, Chen D, Li XF, Ma NH, Wang HW (2009) Electrochemical corrosion behavior of Al–Si alloy composites reinforced with in situ Tib2 particulate. Mater Corros 60:419

[27] Włodarczyk-Fligier A, Dobrzanski LA, Adamiak M (2007) Influence of heat treatment on corrosion resistance of PM composite materials. J Achiev Mater Manuf Eng 24:127

Figures

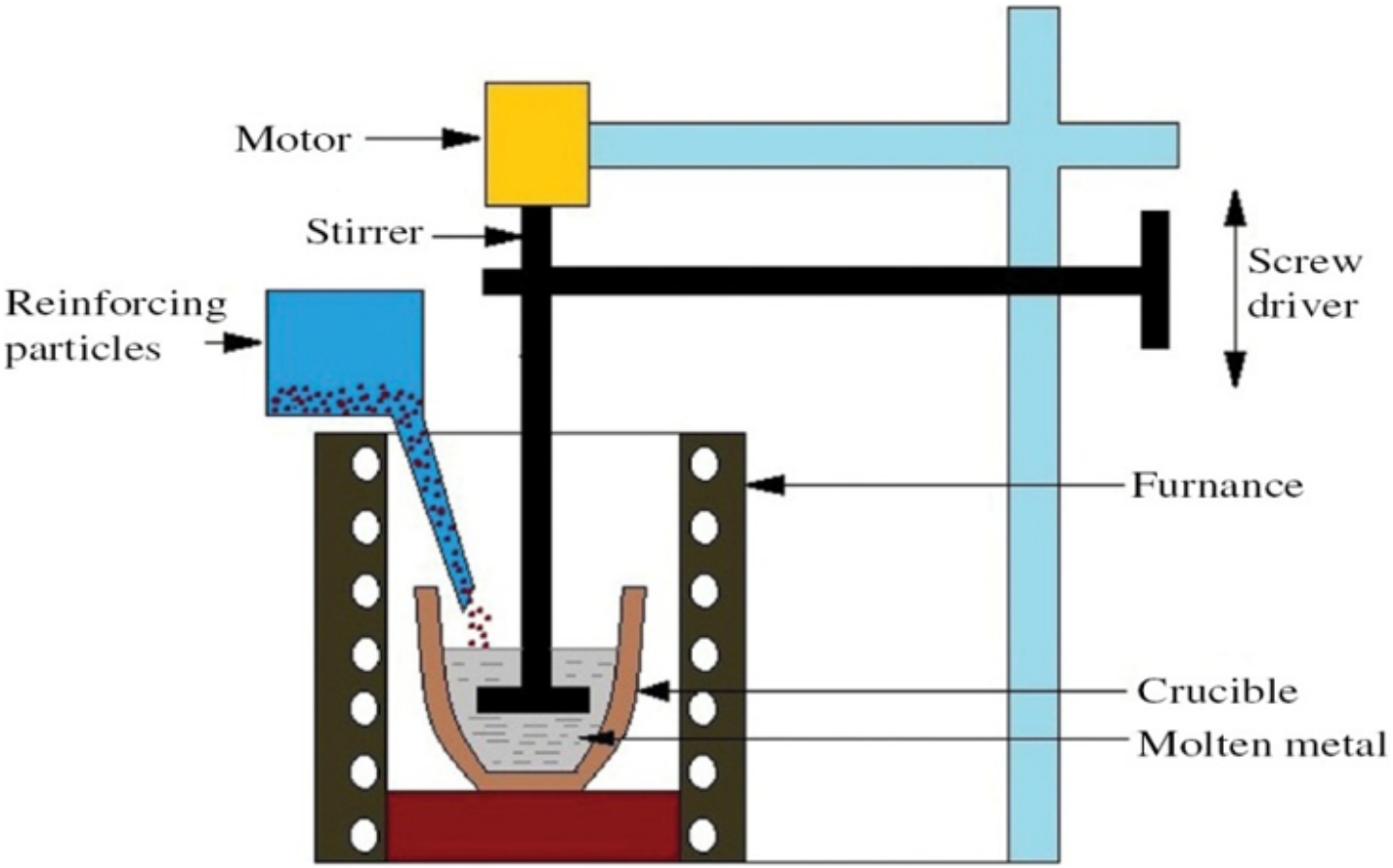

Figure 1

Typical stir-casting Experimental setup

a *b*

Figure 2

Tensile test specimen before testing (a) and after testing (b)

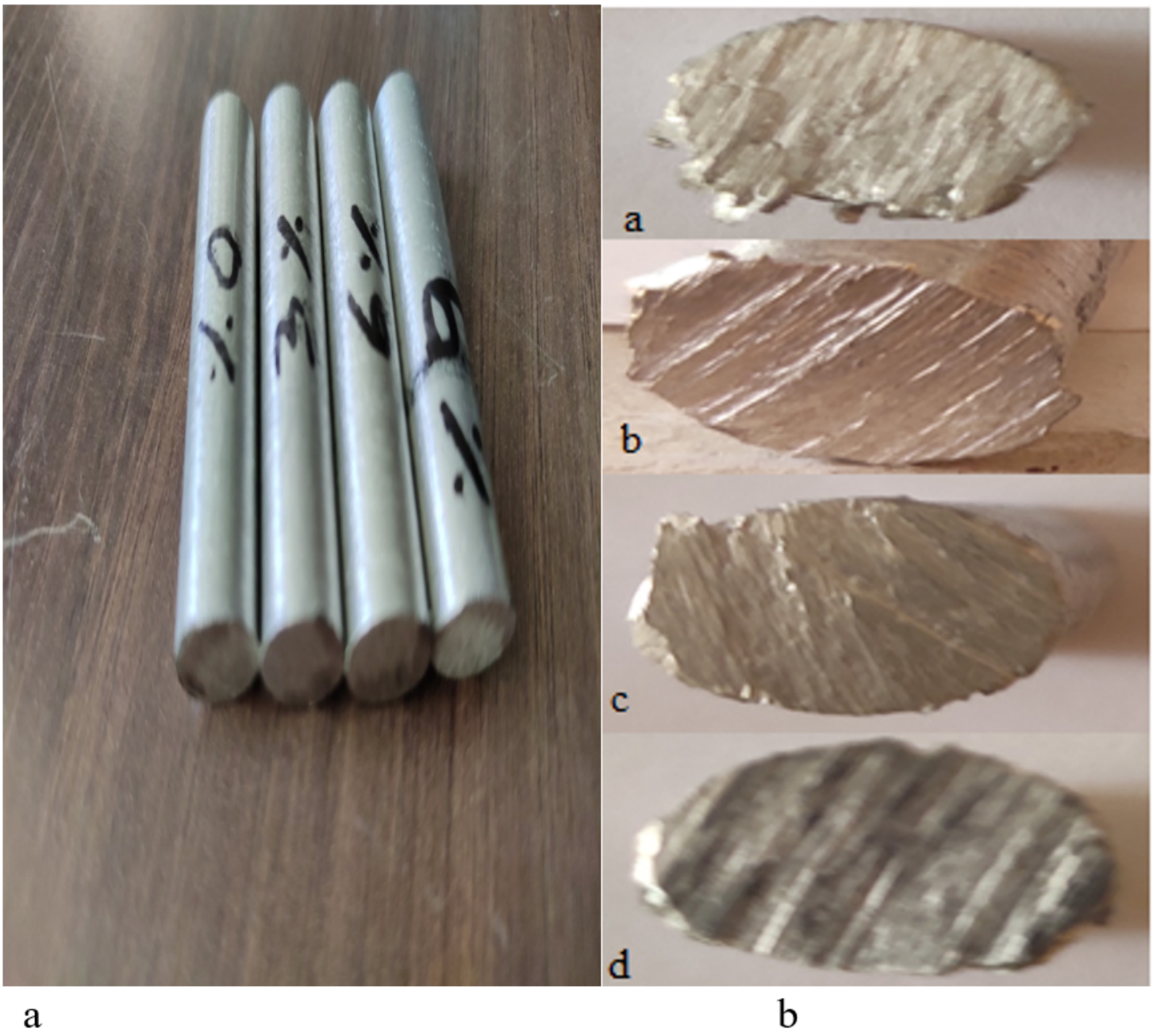

Figure 3

wear specimens (a) Before & (b) After test

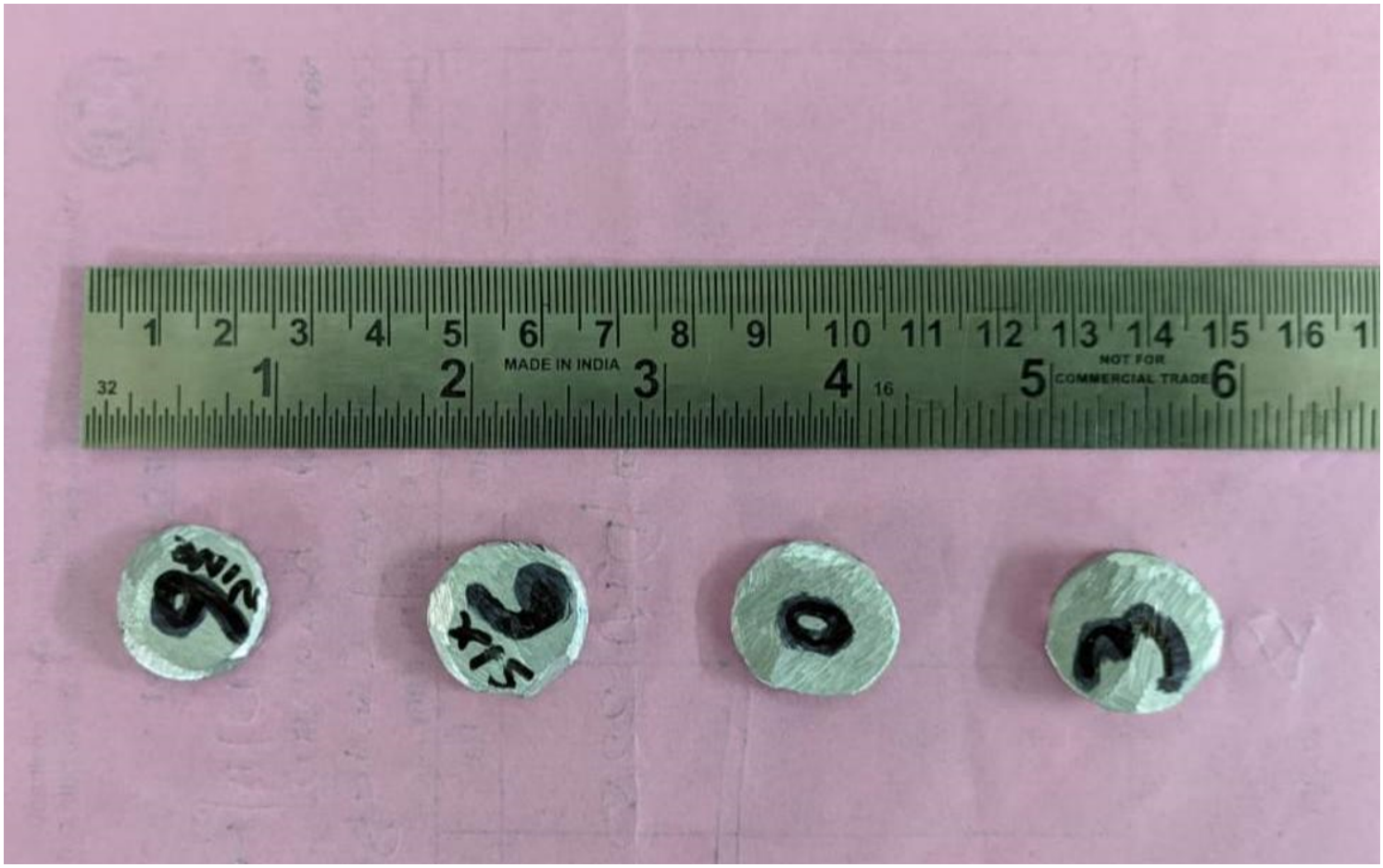

Figure 4

Corrosion samples

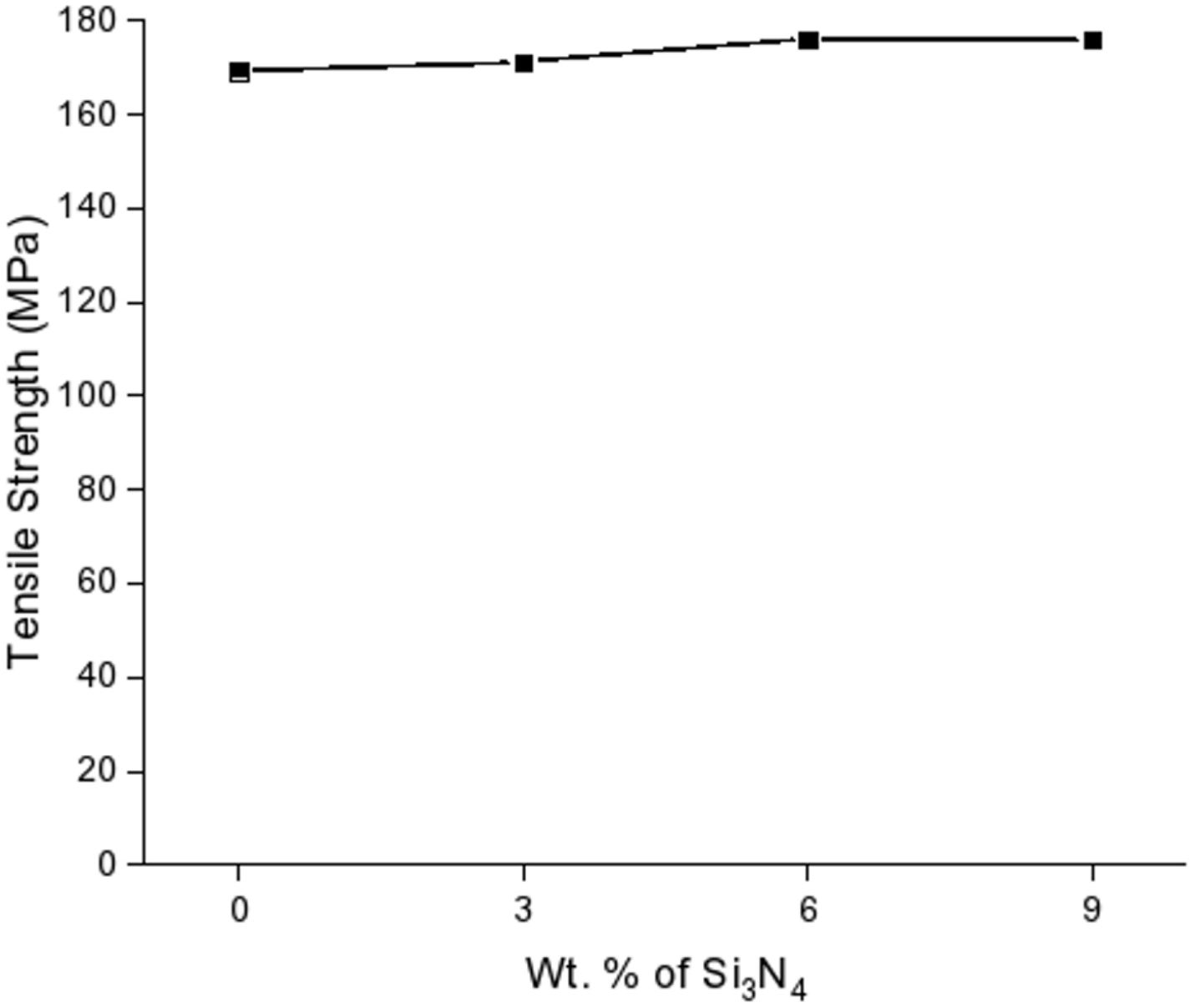

Figure 5

Effect of tensile strength on wt. % of Si3N4

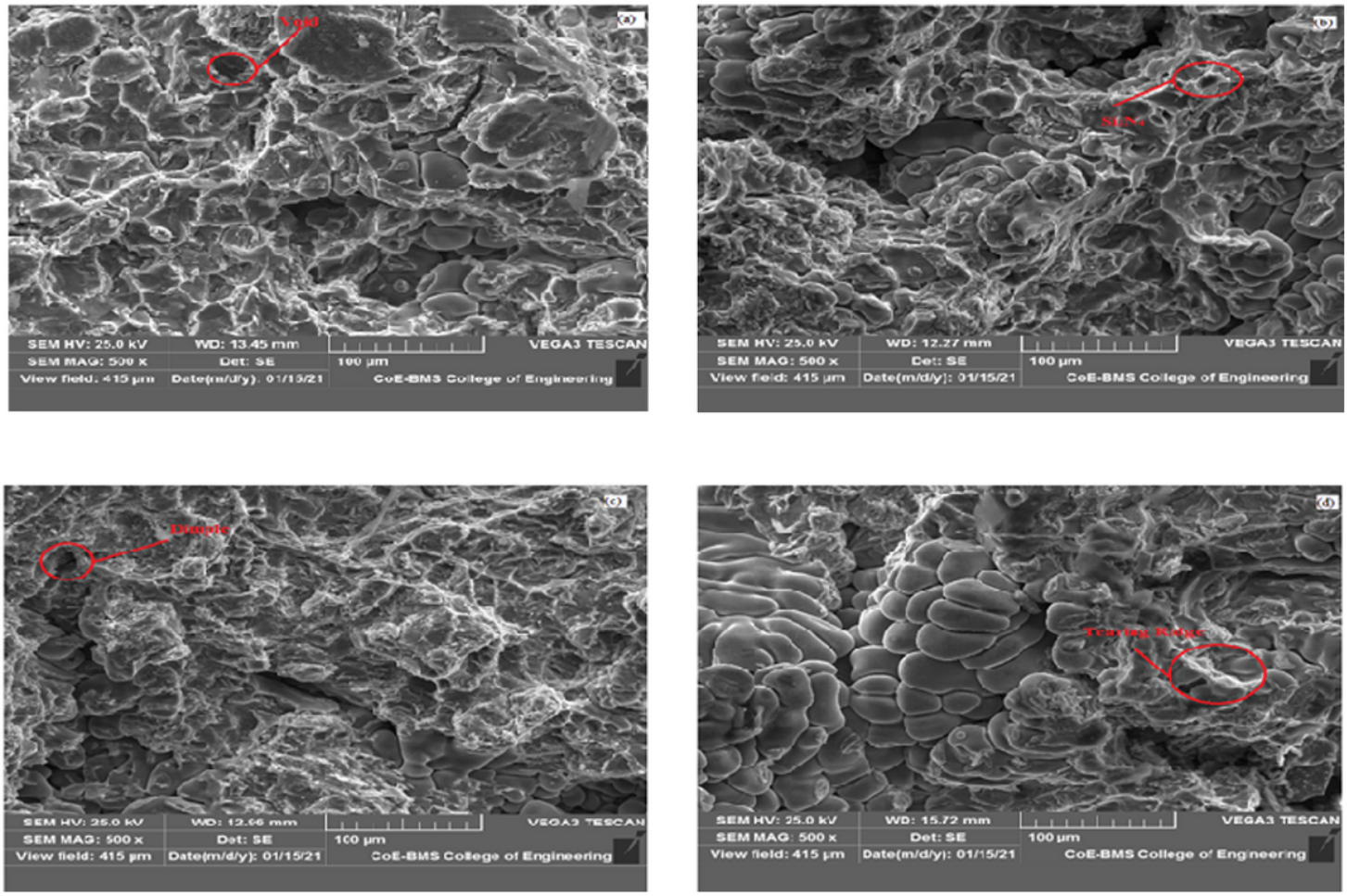

Figure 6

(i): Fractography of Al 2219 Alloy +0% Si3N4 (ii): Fractography of Al 2219 Alloy +3% Si3N4 (iii): Fractography of Al 2219 Alloy +6% Si3N4 (iv): Fractography of Al 2219 Alloy +9% Si3N4

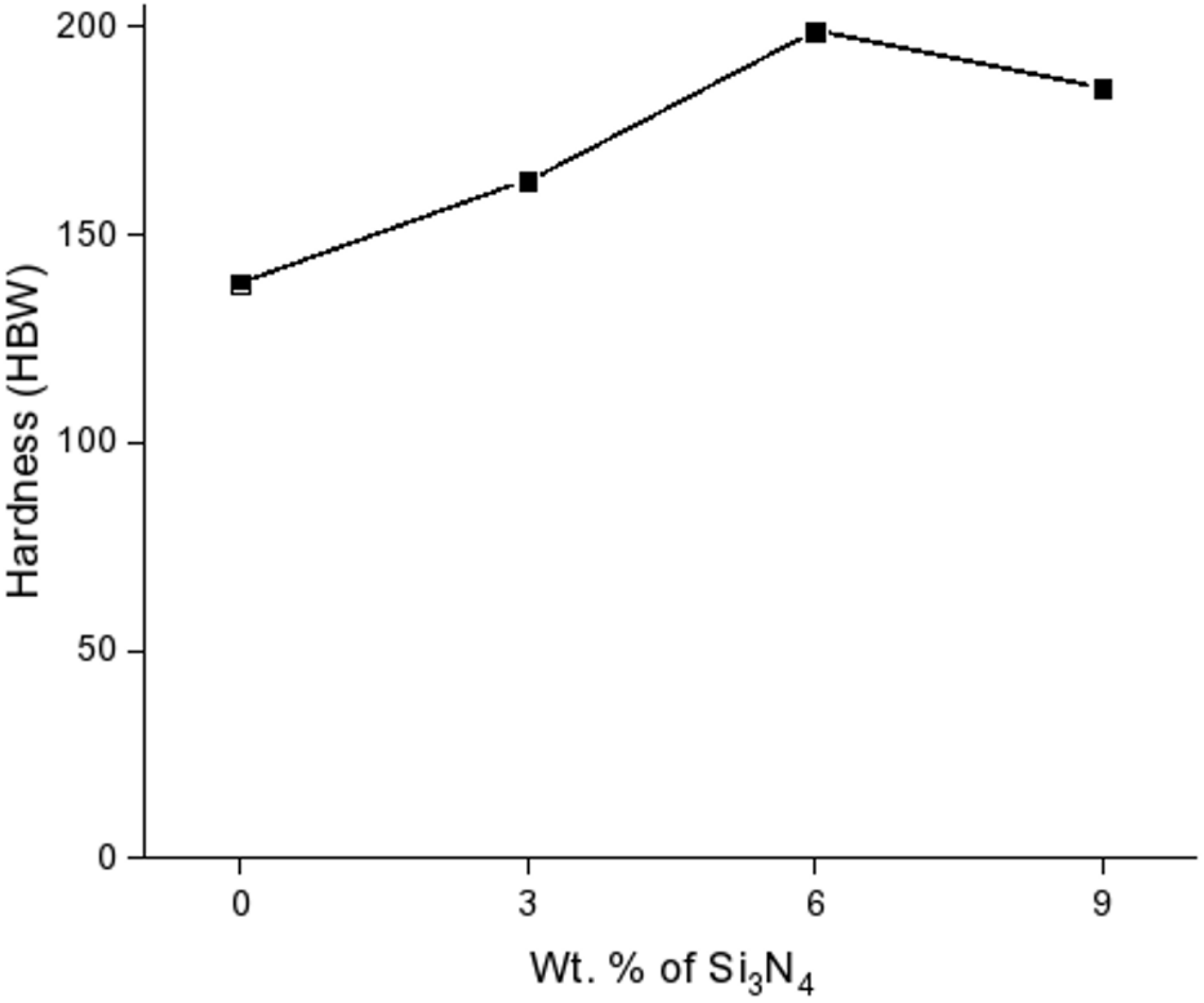

Figure 7

Effect of hardness on wt. % of Si3N4 particles

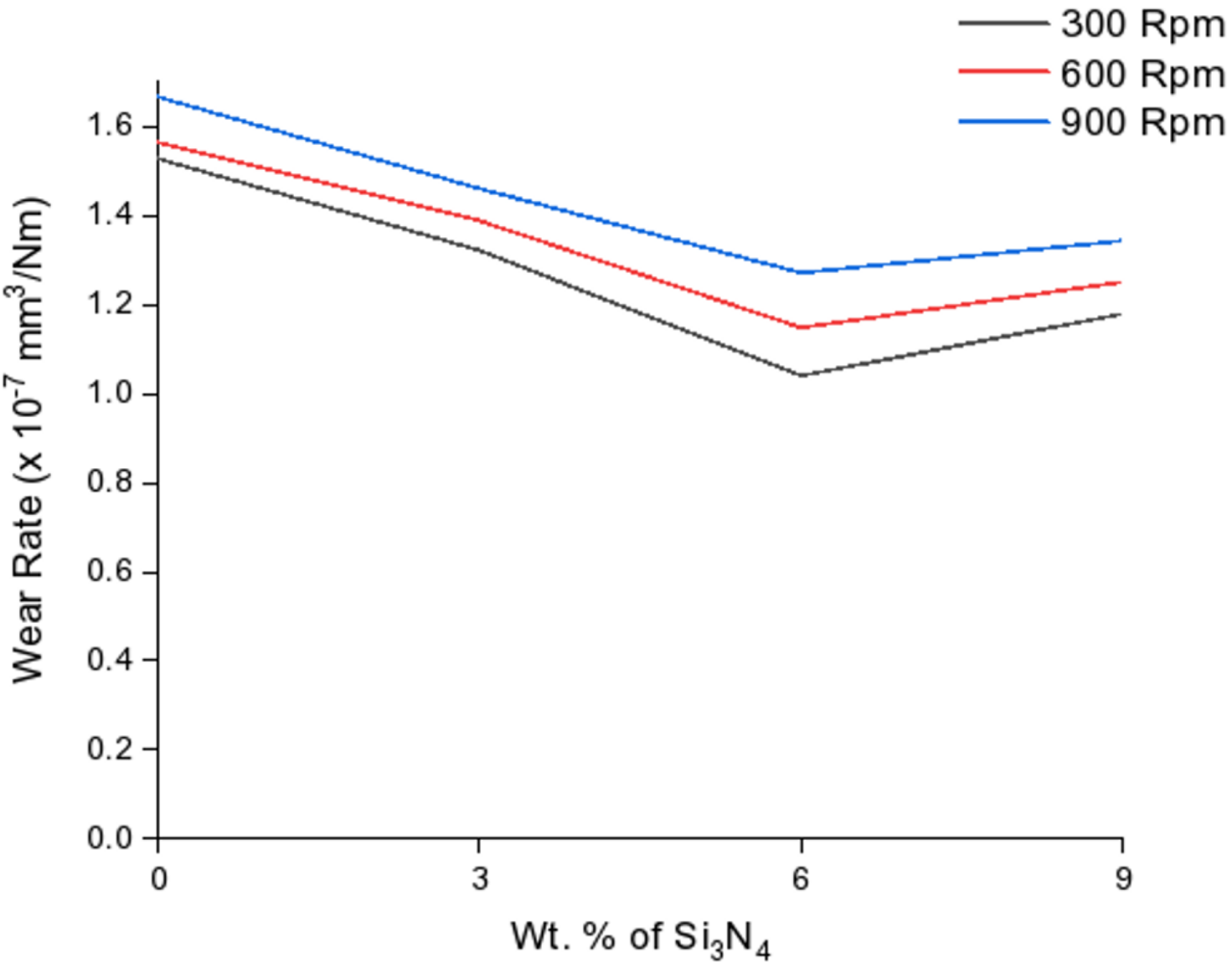

Figure 8

Wear rate vs Wt. % of Si3N4 (load: 20N).

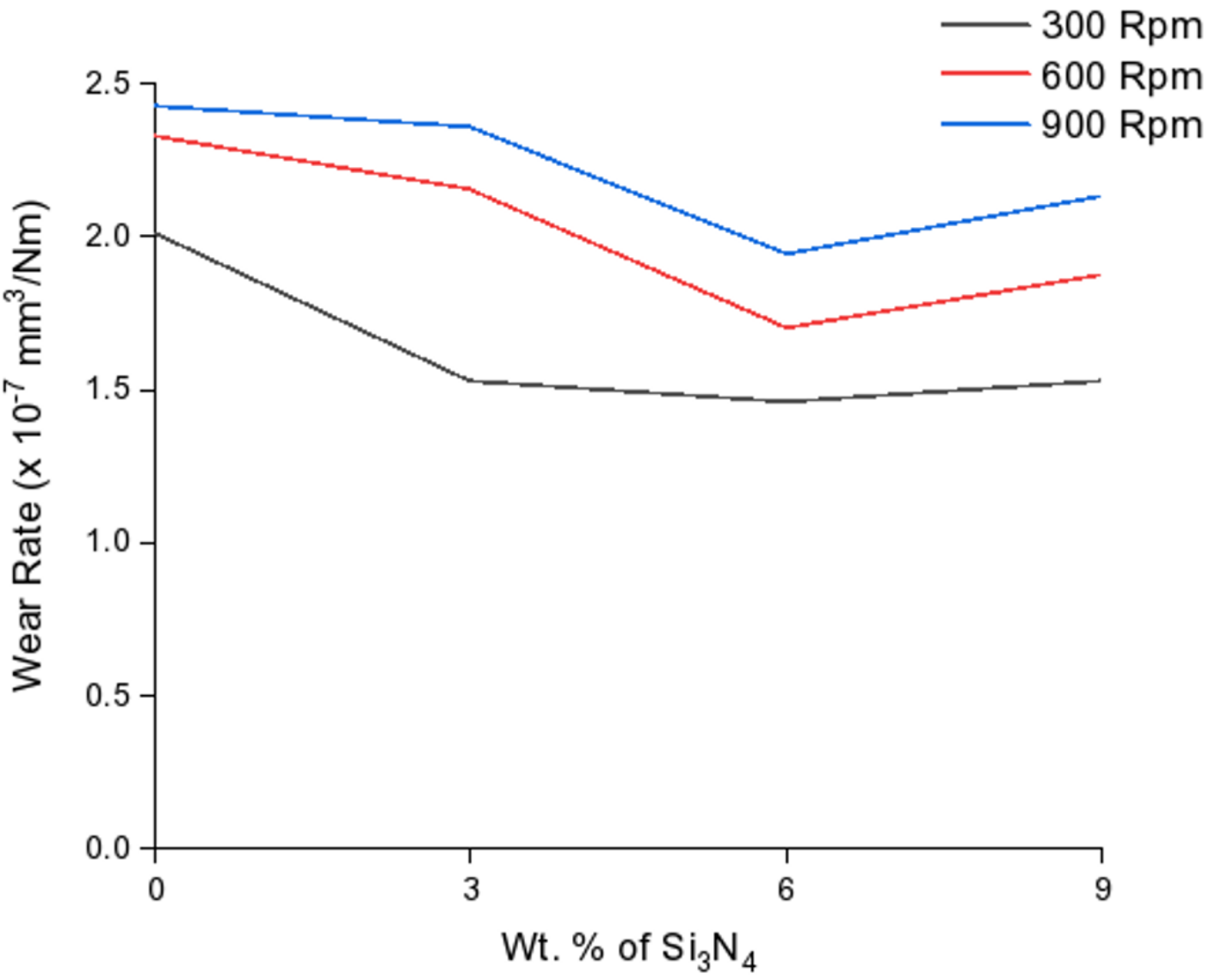

Figure 9

Wear rate vs Wt. % of Si3N4 (load: 40N).

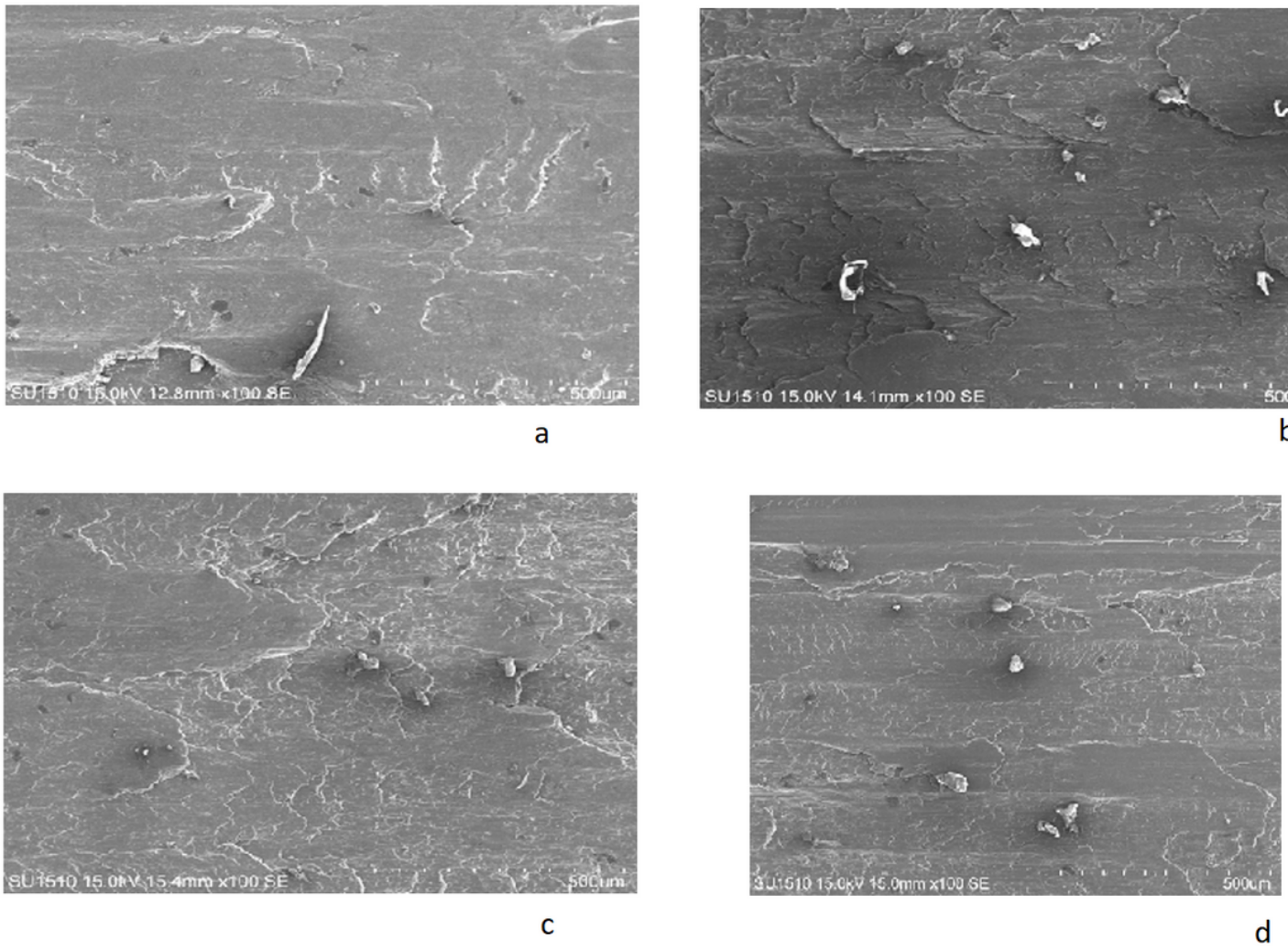

Figure 10

(a): SEM micrographs of the worn surface of specimen for 0% (b): SEM micrographs of the worn surface of specimen for 3% (c): SEM micrographs of the worn surface of specimen for 6% (d): SEM micrographs of the worn surface of specimen for 9%

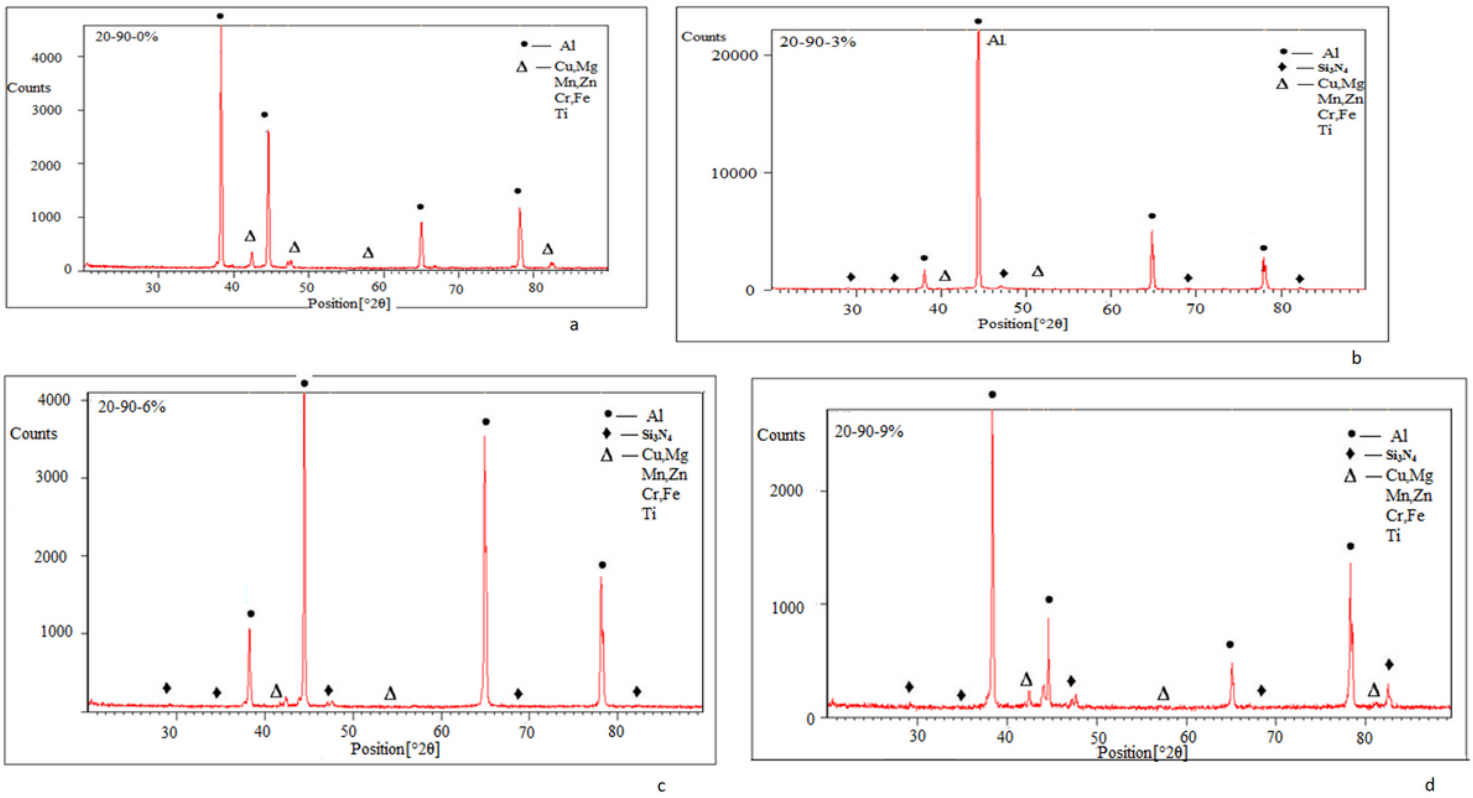

Figure 11

(a): XRD pattern of as casted AA2219 (0%) (b): XRD pattern of AA2219+3 wt % Si3N4. (c): XRD pattern of AA2219+6 wt % Si3N4. (d): XRD consequence ofAA2219+9 wt % Si3N4.

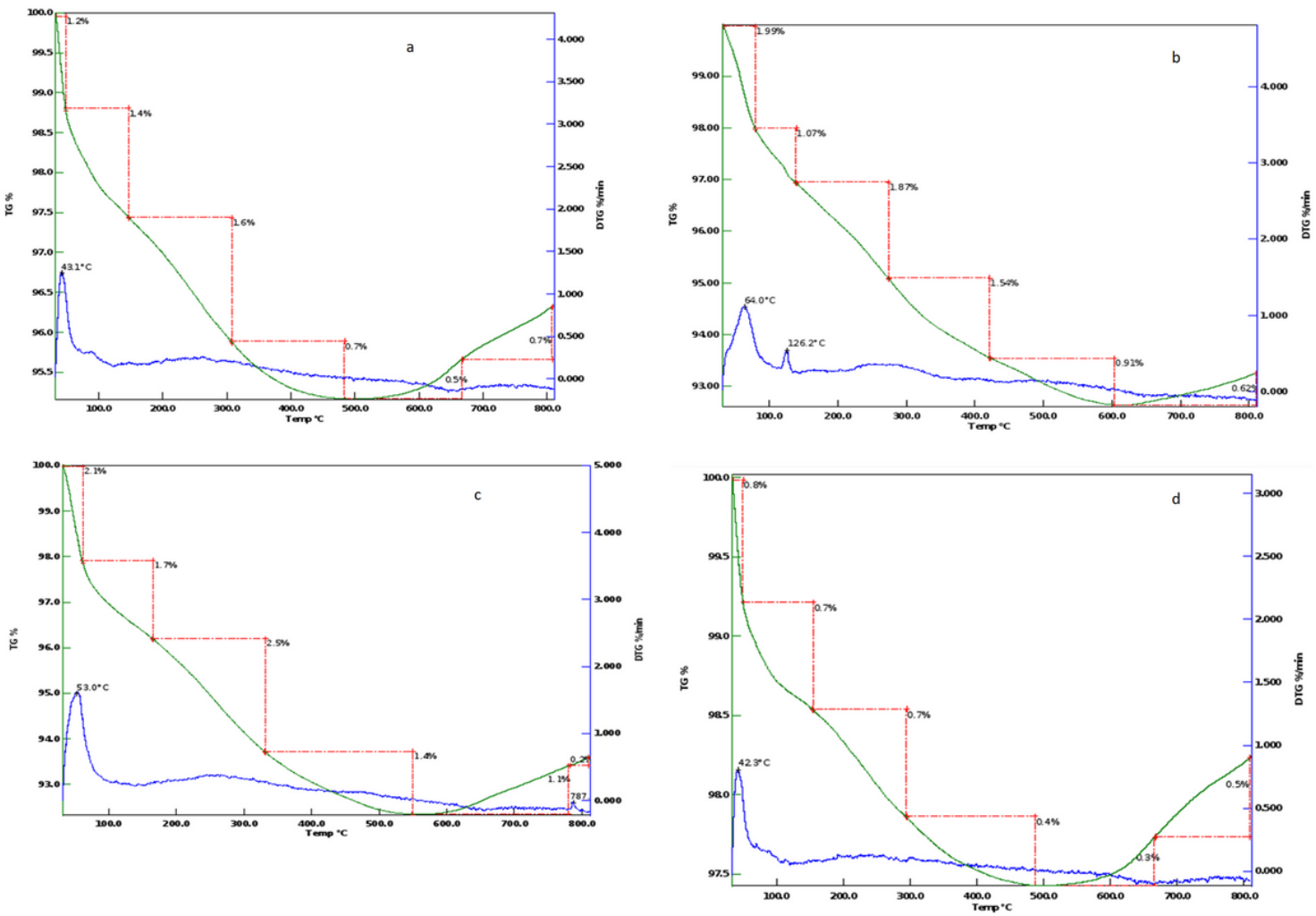

Figure 12

(a): TGA/DTG ofAA2219+0 wt % Si3N4 (b): TGA/DTG ofAA2219+ 3wt % Si3N4 (c): TGA/DTG ofAA2219+6 wt % Si3N4 (d): TGA/DTG ofAA2219+9 wt % Si3N

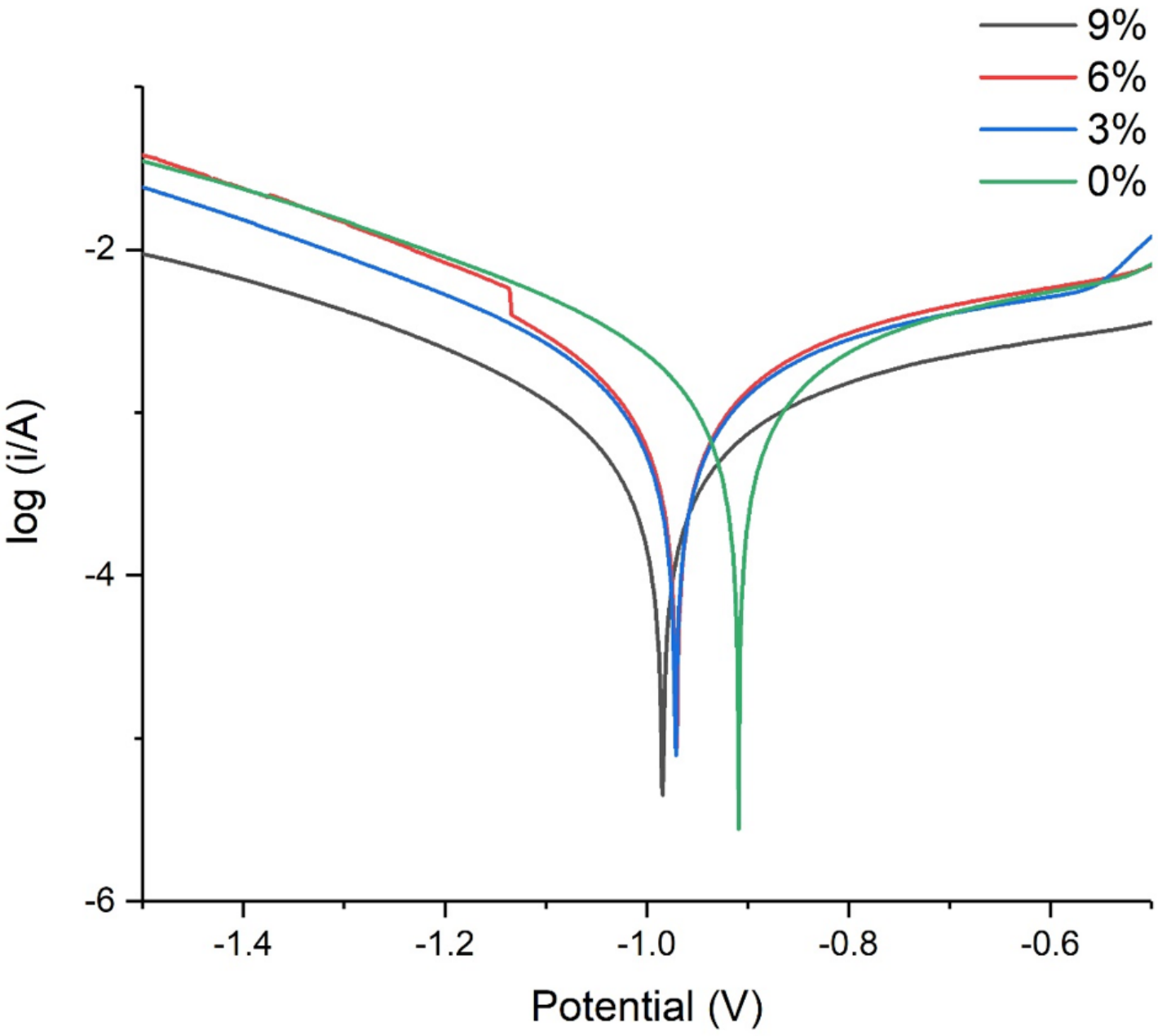

Figure 13

Polarization curves for Al– Si3N4 alloy matrix and its composites with different wt% of Al2O3 particles tested in 3.5 % NaCl